

# Characterization of major lipid droplet proteins from *Dunaliella*

Lital Davidi · Adriana Katz · Uri Pick

Received: 8 September 2011 / Accepted: 29 December 2011 / Published online: 10 January 2012  
© Springer-Verlag 2012

**Abstract** Many green algal species can accumulate large amounts of triacylglycerides (TAG) under nutrient deprivation, making them a potential source for production of biodiesel. TAG are organized in cytoplasmic lipid bodies, which contain a major lipid droplet protein termed MLDP. Green algae MLDP differ in sequence from plant oleosins and from animal perilipins, and their structure and function are not clear. In this study, we describe the isolation of MLDP from three species of the extreme halotolerant green algae *Dunaliella*. Sequence alignment with other green algae MLDP proteins identified a conserved 4-proline domain that may be considered as a signature domain of Volvocales green algae MLDP. Gold immunolabeling localized MLDP at the surface of lipid droplets in *D. salina*. The induction of MLDP by nitrogen deprivation is kinetically correlated with TAG accumulation, and inhibition of TAG biosynthesis impairs MLDP accumulation suggesting that MLDP induction is co-regulated with TAG accumulation. These results can lead to a better understanding of the structure and function of Volvocales green algae MLDP proteins.

**Keywords** *Dunaliella* · Lipid droplets · Lipid droplet protein · Nitrogen deprivation · Triacylglycerides · Volvocales

## Abbreviations

AA Amino acids  
DMF Dimethylformamide  
EDTA Ethylenediaminetetraacetic acid

GRAVY Grand average of hydropathy value  
GSP Gene-specific primers  
NGSP Nested gene-specific primers  
KLH Keyhole limpet haemocyanin  
MLDP Major lipid droplet protein  
NR Nile red  
PAGE Polyacrylamide gel electrophoresis  
PAT Perilipin, adipophilin, TIP47, S3-12 and OXPAT  
PBS Phosphate buffered saline  
RACE Rapid amplification of the cDNA ends  
RFU Relative fluorescence units  
SDS Sodium dodecylsulfate  
TAG Triacylglycerides  
TLC Thin-layer chromatography

## Introduction

Most eukaryotes, including animals, plants yeast and fungi can accumulate lipids in their cells in the form of cytoplasmic lipid droplets. The lipid droplets comprises neutral lipid core surrounded by a phospholipid monolayer embedded with small amount of proteins (Zweytick et al. 2000). Microalgae can accumulate high amount of TAG in response to stress condition or to nutrient limitation, mainly nitrogen deprivation (Shifrin and Chisholm 1981; Roessler 1990; Avron and Ben-Amotz 1992; Thompson 1996). These TAG can be exploited for biodiesel production (Hu et al. 2008; Rodolfi et al. 2009).

The halotolerant alga *Dunaliella* has a relatively high content of omega 3 fatty acid, mainly C18:3 $\omega$ 3 and C16:4 $\omega$ 3 (Abd El-Baky et al. 2004), and its total lipid content may vary from 15 to 40% (Huesemann and Benemann 2009). Moreover, two species of *Dunaliella*, *D. salina* Teodoresco and *D. bardawil*, accumulate under high light or

L. Davidi · A. Katz · U. Pick (✉)  
Department of Biological Chemistry,  
The Weizmann Institute of Science,  
Rehovot 76100, Israel  
e-mail: uri.pick@weizmann.ac.il

nutrient deprivation  $\beta$ -carotene amounting to 10% of their dry weight (Avron and Ben-Amotz 1992). Most of the accumulated TAG are in the form of cytoplasmic lipid droplets, whereas  $\beta$ -carotene accumulates in a different type of plastidic lipid droplets, containing also TAG. The special advantage of *D. salina* as a potential source for biodiesel production is its ability to grow in high salt concentrations and the extended experience in mass cultivation in open raceways (Schenk et al. 2008). However, not much is known about oil metabolism of algae in general and *D. salina* in particular. The proteins associated with *D. salina* lipid droplets have not been characterized.

Lipid droplet proteins have been best characterized in plant seeds and in mammals (Zweytick et al. 2000; Murphy 2001). Plant seeds lipid droplets contain two major proteins, oleosins and caleosins (Tzen and Huang 1992; Murphy 1993; Purkrtova et al. 2008). These proteins have a characteristic hair-pin structure, comprised of a hydrophobic core with a conserved “proline knot”, and hydrophilic N and C terminals (Huang 1992). The proposed function of these proteins is to stabilize lipid droplets by preventing their coalescence with adjacent globules (Huang 1996; Hsieh and Huang 2004). An additional function may be to control TAG lipolysis (Frandsen et al. 2001). Knockout or silencing of plant oleosins was shown to affect the size and number of accumulated lipid droplets in seeds (Siloto et al. 2006; Schmidt and Herman 2008), whereas over-expression of a plant caleosin (AtClo1) in yeast, led to increase in lipid accumulation (Froissard et al. 2009). These results indicate that lipid droplet proteins may control the level and form of TAG accumulation. The major proteins of animal lipid droplets belong to different gene family—the PAT protein family, which has no orthologs in plant seed oil (Murphy 2001; Bickel et al. 2009). Despite their structural differences, plant oleosins and animal PAT family proteins seem to serve similar roles in contributing to lipid droplet stability and preventing their coalescence (Zweytick et al. 2000; Frandsen et al. 2001). Moreover, there is an emerging view that lipid droplets do not serve just for storage of lipid, but they are dynamic organelles that are functionally connected to a variety of organelles and cellular processes (Ducharme and Bickel 2008; Guo et al. 2008).

Until very recently, there was hardly any knowledge about the biogenesis of oil bodies and on the nature of their proteins in microalgae. A recent study in the model green algae *Chlamydomonas reinhardtii* showed that a major lipid droplet protein (MLDP) was the main protein in the lipid droplets (Moellering and Benning 2010; James et al. 2011). We have recently cloned a similar protein from lipid droplets of the astaxanthin-accumulating green alga, *Haematococcus pluvialis* (Peled et al. 2011). Surprisingly, these proteins show no sequence or structural resemblance neither to plant oleosins/caleosins nor to animal perilipins.

In this study, we report the isolation and identification of MLDP from three *Dunaliella* strains. We show that these proteins have high homology to other green algal MLDPs, we identified a highly conserved proline-rich domain in their C-terminal end and we demonstrate a high correlation between *D. salina* MLDP expression and oil accumulation.

## Materials and methods

### Strain and growth condition

*Dunaliella salina* (a green species) was obtained from Dr. W. H. Thomas, La Jolla, CA, USA (Ben-Amotz et al. 1982). *Dunaliella bardawill* is an isolated species (Ben-Amotz et al. 1989) deposited at the American Type Culture Collection (ATCC), Rockville, MD, USA, No. 30861. *Dunaliella parva* Lerche 19/9 was obtained from the Cambridge culture collection. Culturing conditions and growth media of all *Dunaliella* species were as previously described (Ben-Amotz et al. 1989). The media were supplemented with 2 M NaCl (*D. salina*, *D. bardawill*) or with 1 M NaCl (*D. parva*). To induce N limitation, mid-log-phase cells were centrifuged for 5 min at 5,000 g, washed once with growth medium lacking KNO<sub>3</sub> (–N medium), and re-suspended in –N medium. Cells were counted with the automated cell counter Cellometer (Nexelom Bioscience LLC, Lawrence, MA, USA).

### Lipid droplets isolation

Isolation of globules was performed essentially as previously described with some modifications (Jiménez and Pick 1994). In brief, algae were ruptured osmotically and then centrifuged at low speed for elimination of chloroplasts. Control (nitrogen sufficient) cells were ruptured in the presence of synthetic lipid globules, prepared by sonication of 100  $\mu$ l Triolein with 0.1% phosphatidylcholine in 50 mM Tricine buffer containing 1 mM EDTA. Purification of the globules was performed by flotation on a discontinuous sucrose gradient consisting of three layers (30% sucrose containing the globule fraction; 15% sucrose and 5% sucrose, all containing 10 mM Tris–HCl, pH 8) and centrifugation at 75,000 g for 2 h. The crude globules, recovered from the top fraction, were collected and re-purified by flotation on a second sucrose gradient. The purified globules were collected from the top and kept frozen in liquid nitrogen.

### Mass spectrometric identification of *D. salina* major lipid droplet proteins

Proteins were precipitated overnight in 80% acetone at –20°C. The pellet was re-suspended in sodium dodecyl

sulfate (SDS) sample buffer without reducing agent and dye. Protein content was assayed by the bicinchoninic acid method (Sigma-Aldrich, St. Louis, MO, USA), the reducing agent, and the dye were added and incubated for 2 min at 90°C. Proteins were separated on 12% SDS–PAGE gels and stained with 0.25% Coomassie blue in 50% methanol and 10% acetic acid reagent. The band containing the major protein was cut-out and processed for analysis by liquid chromatography–tandem mass spectrometry (LC–MS/MS) at the core research facility in the Hebrew university of Jerusalem. Protein sequences with over 50% confidence filter were considered true.

#### Cloning the putative *D. salina* MLDP

On the basis of MS–MS results, degenerate oligonucleotide primers were designed: DS deg F: 5′-TGGGCNGTNGARA AYYT, DS deg R: 5′-TCNGCNACNGGYTGNAC. PCR with these primers revealed a 356-bp nucleotide band which was sequenced and cloned. This sequence (designated DS conserved) showed high homology to *Chlamydomonas reinhardtii* MLDP (Moellering and Benning 2010). To generate the full-length cDNA of the putative *D. salina* MLDP, 3′ and 5′ rapid amplification of the cDNA ends (RACE) was performed using a BD smart RACE cDNA Amplification Kit (BD Biosciences Clontech, Foster City, CA, USA), according to the manufacturer's manual. To amplify the 5′ end, the reverse gene-specific primers (GSP1) 5′-GCCAGCGGTCTCTCAGTGAAGTTGA and the nested (NGSP1) 5′-ATAGTGTGTCAGGGTCC were designed using Amplify3 software. To amplify the 3′ end, the forward gene-specific primers (GSP2) 5′-GGAACATCTTCTACGCGCTACATGAC and the nested (NGSP1) 5′-AGTTTGCTGTGGACTC were constructed to amplify the 3′ end of the target gene. RACE PCR reactions were conducted using 5′ and 3′-RACE-Ready cDNAs made from 1 µg total RNA of N-starved cells with SMARTScribe Reverse Transcriptase (Clontech Laboratories). The PCR products of the expected size were excised from the gel and purified (ZymoClean gel DNA recovery kit; Zymoresearch, Irvine, CA, USA). The full-length cDNA corresponding to the *D. salina* putative MLDP was assembled from DS conserved together with the 5′ and 3′ RACE fragments. Putative MLDPs from *D. parva* and *D. bardawil* were cloned in the same way.

#### Generation of anti-MLDP antibodies

Polyclonal antibodies were raised in rabbits as follows: On the basis of the amino acid MLDP sequence, using IEDB Epitope Prediction and Analysis Tool software (<http://www.tools.immuneepitope.org/main>), four putative antibody sequences were selected. These peptide sequences were chemically synthesized (peptide synthesis service

laboratory, Weizmann Institute, Rehovot), and conjugated to Inject Maleimide-activated Keyhole limpet haemocyanine (mcKLH, Pierce, Rockford, IL, USA), according to the manufacturers' instruction. The KLH-conjugated peptides were injected into rabbits and the serum was collected and kept at –20°C. The only peptide that gave specific result is (C)NSTLDYWKPNT. This peptide is the one used in this work.

#### Gel electrophoresis and immunoblot analysis

Protein extracts from total cells were generated from pellets of culture samples containing  $2 \times 10^6$  cells re-suspended in 0.1 ml of bursting solution (5 mM Hepes, pH 7.5, 5 mM  $\gamma$ -caproic acid, 1 mM benzamidine, 1 mM PMSF), followed by the addition of 50 µl of sodium dodecyl sulfate (SDS) sample buffer. Protein extracts from total cells, or from isolated globules were analyzed by 12% SDS–PAGE acrylamide as indicated. Gels were stained with 0.25% Coomassie blue in 50% methanol and 10% acetic acid or immunoblotted with anti-MLDP antibodies. Proteins were transferred to nitrocellulose and then the blot was incubated overnight at 4°C with PBS, 0.05% Tween, and 10% low-fat milk (T-PBS milk buffer). The blot was incubated for 1 h at room temperature with anti-MLDP antibodies at a dilution of 1:1,000 in T-PBS buffer and washed extensively with T-PBS milk buffer. The blot was incubated at room temperature for 1 h with anti-rabbit IgG peroxidase conjugate diluted 1:20,000 in T-PBS and then washed in the same buffer. Bound antibodies were detected with the ECL (enhanced chemiluminescence) detection system (homemade, using  $\gamma$ -caproic acid and luminol of Sigma-Aldrich (St. Louis, MO, USA).

#### cDNA preparation

Cells for RNA isolation were harvested from 10 ml log-phase culture (time 0) grown in complete medium and cultured on nitrogen-free medium for 24, 32, 48, 72, 96, 168 h. The cells were collected by centrifugation and immediately flash-frozen in liquid nitrogen and stored at –80°C for further use. Total RNA was isolated using tri-reagent procedure according to manufacture protocol (Molecular Research Center, Cincinnati, OH, USA). Independent RNA isolations were conducted for each growth period. Template cDNA was synthesized using 0.1 µg total RNA in a total volume of 20 µl, using Superscript kit (Invitrogen, Carlsbad, CA, USA). MLDP gene expression of *D. salina* N-deprived cells was examined using MLDP gene primers (F:5′-CCAAGGGTGAGCGGTTTGT, R:5′-CCTCACAGAGTTTCATC) and was compared with the expression of 18S control gene.

## TAG and fatty acid analysis

For TAG quantification two methods were used: specific Nile red (NR) fluorescence in live cells and thin-layer chromatography (TLC) in cell extracts. NR was added to live cells ( $10^6$  cells/ml) in the fresh growth medium or purified lipid droplets (normalized to cell concentration of  $10^6$  cells/ml), at a final concentration of 1  $\mu$ M (from 1 mM stock in DMF). The fluorescence emission was measured after 3–10 min, when the signal reached maximal and steady level, according to NR kinetics, determined separately for each algae species. The parameters of NR fluorescence measurement: excitation at 488 nm, emission at 580–590 nm (the peak of neutral lipids). The increase in fluorescence emission was utilized to express the relative increase in TAG level. For the TLC analysis, lipids were extracted from  $2.5 \times 10^7$  cells as previously described (Khozin-Goldberg et al. 2005), separated on TLC Silica gel 60 aluminum sheets (Merck, Darmstadt, Germany) in n-hexane: diethyl-ether: acetate (85:15:1, by vol.) solution, and finally lipid detection was performed by 5 min exposure to iodine vapor. For quantification, densitometric analysis of spots was compared with standards of 0.5–2  $\mu$ g triolein. Chlorophyll and carotenoid contents of *D. salina* control and N-deprived cells or of purified lipid droplets were determined in lipid extracts from the absorbance at 663 and 480 nm, respectively.

For GC/MS analysis of fatty acid composition and total lipid contents, lipids were extracted from 50 ml cells ( $5 \times 10^6$  cells/ml) and 2 ml of purified globules. Total fatty acid methyl esters (FAME) were prepared through acid hydrolysis in methanol and then analyzed by GC/MS (performed by Dr. Inna Khozin-Goldberg, Prof. Zvi Cohen's lab in Ben-Gurion University). Three replicates or each sample were examined.

## Confocal microscopy analysis

For confocal microscopy analysis, cells were fixed in 2.5% glutaraldehyde, stained with 1  $\mu$ M NR (from 1 mM stock in DMF) followed by 1 min incubation in the dark and applied to the microscope slide. Images were captured using Olympus FlowView 1000 microscope (Olympus, Center Valley, PA, USA). Excitation was provided by a 559 nm and a 638 nm diode lasers. Nile red fluorescence (to detect lipid droplets) was followed using 559 nm laser and a 575–620 nm emission filter and chlorophyll autofluorescence was monitored by using 638 nm laser and a 660–753 nm emission filter.

## Gold immunolabeling

Cells grown in complete or in N-deprived medium for 3 days were fixed in 2% glutaraldehyde and 0.1% acrolein. The fixed cells were gelatinized, cryosectioned, and labeled

with anti-MLDP antibodies (dilution of 1:150) followed by incubation with 10 nm gold-conjugated goat antirabbit IgG. Grids were stained with uranyl acetate. Transmission electron micrographs were captured using FEI 120 kW TEM and FEI eagle 2 k  $\times$  2 k CCD camera (FEI, Eindhoven, The Netherlands).

## Bioinformatics

Sequences were routinely searched using BLAST (Altschul et al. 1997). Sequences were aligned using the Tcoffee multiple sequence alignment program (Goujon et al. 2010). Hydrophathy plots were generated employing the Kyte–Doolittle algorithm (Kyte and Doolittle 1982), using the ProtScale program at <http://www.expasy.ch/tools/protscale.html>. The value *G* in each graph is the grand average of hydrophathy value (GRAVY) for each protein and was calculated using the GRAVY calculator program at <http://www.gravy.laborfrust.de/>. Post-translational modifications were screened using online software: prenylation: <http://www.mendel.imp.ac.at/sat/PrePS/index.html>, N-myristoylation: <http://www.mendel.imp.ac.at/myristate/SUPLpredictor.htm>, phosphorylation: <http://www.cbs.dtu.dk/services/NetPhos/>, GPI-anchor: <http://www.gpi.unibe.ch/>. Secondary structure prediction were obtained using secondary structure consensus prediction program [http://www.npsa-pbil.ibcp.fr/cgi-bin/npsa\\_automat.pl?page=/NPSA/npsa\\_seccons.html](http://www.npsa-pbil.ibcp.fr/cgi-bin/npsa_automat.pl?page=/NPSA/npsa_seccons.html)

## Results

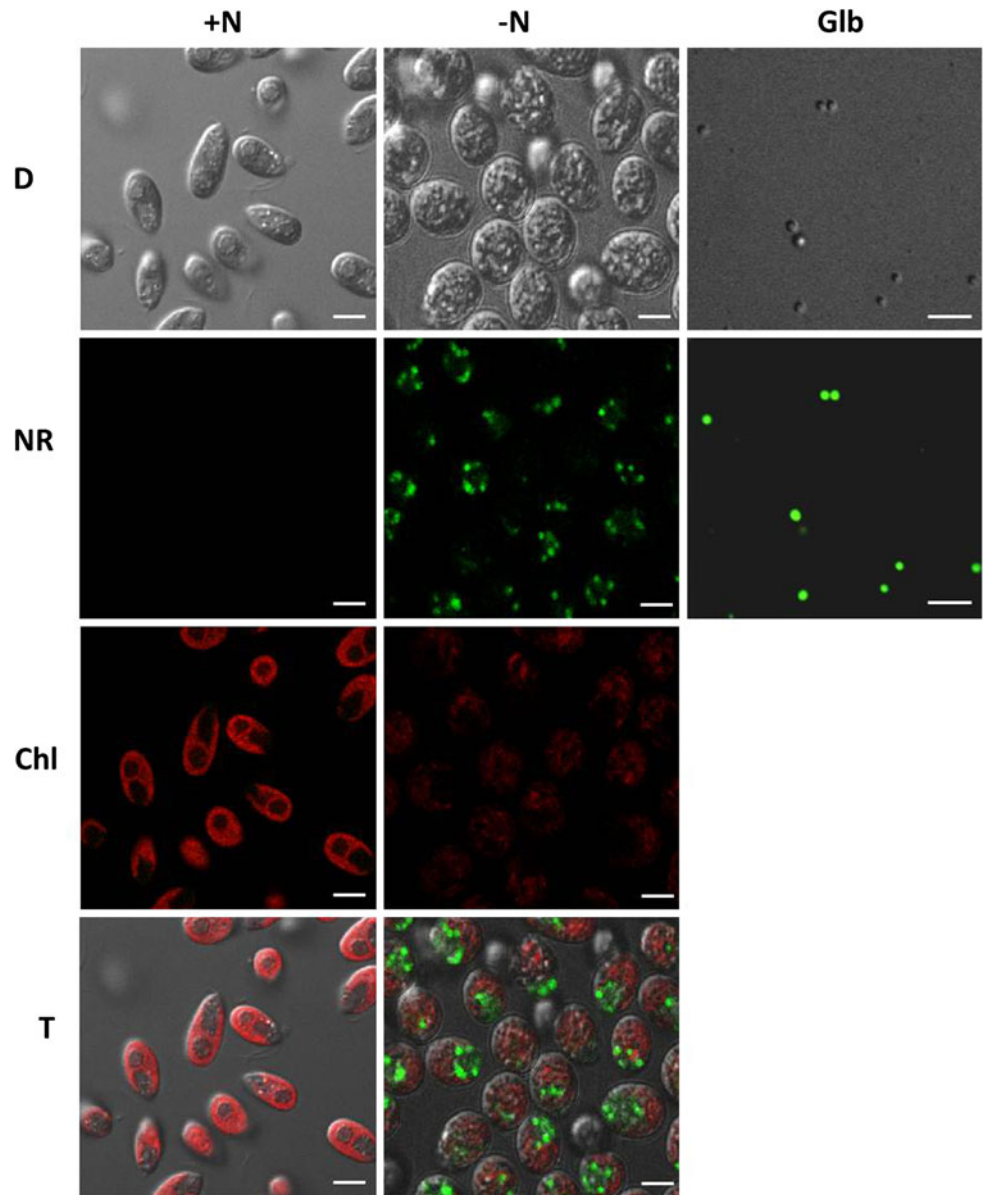
### Accumulation of TAG in N-deprived cells

To visualize TAG accumulation in *D. salina*, cells were deprived of nitrogen (–N), stained with the lipid-sensitive fluorescent dye Nile red (NR), and viewed by confocal microscopy in comparison to control (N-sufficient, +N) cells (Fig. 1). Whereas N-sufficient cells reveal a well-defined cup-shaped chloroplast and no lipid droplets, N-deficient cells were characterized by a fragmented low-fluorescence chloroplast, and by multiple cytoplasmic lipid droplets. The apparent fragmentation of the chloroplast probably reflects the accumulation of large starch granules within the chloroplast of N-deprived cells. The decrease in chlorophyll fluorescence is also presented in the time course of chlorophyll fluorescence during N-deprivation (see Fig. 8b).

### Lipid droplet purification

Dunaliella is an attractive candidate for biochemical analysis in general, and for isolation of lipid droplets in particular, because being a wall-less algae, it can be osmotically

**Fig. 1** Visualization of lipid droplets in *D. salina* by confocal microscopy. Algae were grown for 3 days in complete medium or in N-deficient media. +N *D. salina* cells grown in complete media. -N *D. salina* cells grown in N-deficient media. *Glb* purified globules from *D. salina* N-deficient cells. Confocal images: *green* NR fluorescence, *red* chlorophyll fluorescence. *D* differential interference contrast, *NR* Nile red fluorescence, *Chl* chlorophyll fluorescence, *T* all figures merged. Bars 5 μm



lysed under gentle conditions that keep the chloroplast intact, thus avoiding contamination of lipid droplets with pigments and proteins, a major concern in characterization of lipid droplets from most algae species.

Cytoplasmic lipid droplets were purified by osmotic disruption of the cells followed by floatation on a sucrose density gradient. To trace non-specific contaminations, artificial lipid droplets, composed of triolein and trace phospholipids, were prepared and added to the control (N-sufficient) samples during lipid droplet purification. This technique enabled subsequent identification of non-specific proteins that interact with lipid droplets. Chlorophyll and carotenoids contents in the lipid droplet were also measured. The criteria set for lipid droplet purity were (1) the relative level of polar lipids, representing contamination

by various membranes, (2) absence of chlorophyll and of carotenoids, resulting from ruptured chloroplast, (3) enrichment in fatty acid 18:1ω9 (next paragraph below) and (4) enrichment in the 30 kDa (next section below). Lipid analysis of the isolated lipid droplets extracts by TLC reveals that they contain mostly triglycerides, very little polar lipids and no detectable chlorophyll or carotenoids (Fig. 2a). Nile red staining fluorescence emission spectra of cells and isolated droplets shows the characteristic staining of neutral lipids at 580–590 nm in the N-deprived and isolated droplets, which is absent in control cells, and the chlorophyll emission at 685 nm, which is absent in the lipid droplets (Fig. 2b). Spectrophotometric analysis of pigment contents in the lipid droplets extracts, yielded values of about 0.5% (w/w) carotenoids and no detectable chlorophyll (not

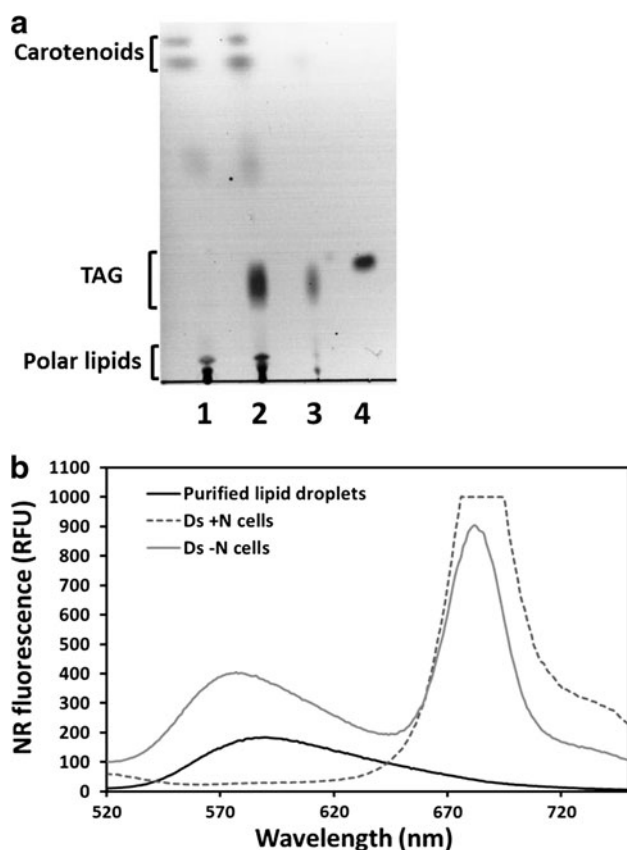


**Fig. 2** TLC and Nile red analysis of isolated lipid droplets. **a** TLC analysis of *D. salina* control cells (lane 1), N-deprived cells (lane 2), purified lipid droplets (lane 3) and 1  $\mu$ g of triolein standard (lane 4). **b** Fluorescence emission spectra of Nile red-stained *D. salina* control cells (Ds + N), N-deprived cells (Ds – N) and purified lipid droplets. TLC and NR analysis were conducted in samples normalized to equal cell number

shown). Estimation of lipid droplet content yields over 90% TAG, less than 10% polar lipids and negligible amounts of pigments, indicating that they are highly purified and contain little if any membrane contaminations. The small amount of polar lipids may represent the monolayer of phospholipids covering the lipid droplet.

Fatty acid composition analysis of *D. salina* cells and lipid droplet was conducted by GC analysis of the FAMES (Table 1). The lipid droplets and N-deprived cells were enriched in the fatty acids 16:0 and 18:1 $\omega$ 9 in comparison to control (N-sufficient) cells, amounting to 50% of the fatty acid content of isolated lipid droplets. These results are in agreement with the previous studies in *C. reinhardtii* which showed elevated levels of 16:0, 18:1 $\Delta$ 9 (also designated 18:1 $\omega$ 9), under N-deprivation (James et al. 2011). In contrast, the levels of the fatty acids 18:3 $\omega$ 3 and 16:4 $\omega$ 3, which are components of the chloroplast thylakoid membrane, decreased in N-deprived cells and more so in lipid droplets, compared to control cells, representing a decrease in chloroplast membrane contents in N-deprived cells. In addition, there is decrease in

**Table 1** Fatty acid composition (%w/w) of *D. salina* cells and lipid droplets

Fatty acid (% of total)	Whole cells		Cytoplasmic globules
	Ds + N	Ds – N	Ds – N
16:0	12.8	22.2	25.6
16:1 $\Delta$ 9	9.2	3.6	1.6
16:1 $\Delta$ 3	1.8	0	0
16:2 $\omega$ 6	1	0.8	0.6
16:3 $\omega$ 3	2.2	2	1.2
16:4 $\omega$ 3	20.2	11.7	6.2
18:0	1.8	1.7	2.2
18:1 $\omega$ 9	3.1	15.3	24.1
18:1 $\omega$ 7	1.2	1.2	1.8
18:2 $\omega$ 6	9.3	12.6	16.3
18:3 $\omega$ 6	2.3	2.2	2.5
18:3 $\omega$ 3	35.1	26.6	17.9

*D. salina* cells were grown in complete (N-sufficient) or in N-deficient media. Lipid droplets were purified after 3 days. Total lipid extracts were prepared from total cells and from purified lipid droplets. Total fatty acid methyl esters (FAME) were prepared through acid hydrolysis in methanol and analyzed by GC/MS

The results represent average values of three repeats

minor fatty acids 16:1 $\Delta$ 3 and 16:1 $\Delta$ 9, which probably are also components of the thylakoid membrane.

#### Identification and characterization of MLDP from *D. salina*

Protein composition analysis of cytoplasmic lipid droplet of *D. salina* was conducted by SDS–PAGE (Fig. 3). Cytoplasmic globules of N-deprived cells were highly enriched with a 30 kDa protein which was not evident in the control sample. This protein band was excised from the gel and was subjected to MS–MS analysis for protein identification. On the basis of the peptides sequences obtained from the MS–MS analysis, degenerate oligonucleotide primers were designed. PCR amplification conducted on cDNA of N-deprived cells as template with these primers revealed a 356 bp band. The band was sequenced and cloned and its putative amino acid sequence showed high homology to *C. reinhardtii* MLDP (Moellering and Benning 2010) (data not shown). To generate the full-length cDNA of the putative *D. salina* MLDP, 3' and 5' rapid amplification of the cDNA ends (RACE) was performed. The cDNA product of 984 bp was obtained with an open reading frame (ORF) of 846 bp (accession number JQ011390). The full-length cDNA sequence, designated *D. salina* MLDP, encoded for a protein with 281 amino acid and molecular weight of 31,110 Da. On the basis of sequence homology, MLDP from *Dunaliella bardawil* and *Dunaliella parva* were sequenced and cloned in the same way (accession numbers

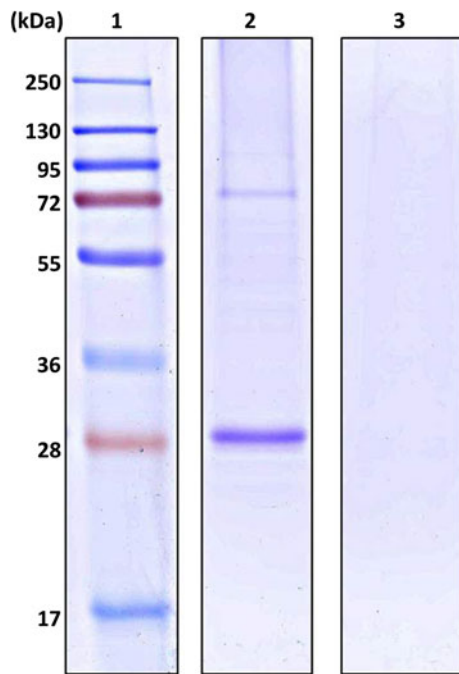


**Fig. 3** SDS-PAGE of *D. salina* lipid droplet proteins. *Lane 1* MW standards, *lane 2* lipid droplet proteins from N-deprived algal cell. *Lane 3* lipid droplet proteins from control (N-sufficient) algal cell. 20 g proteins were loaded in each lane. The results shown are representative of three experiments

JQ011391 and JQ011392, respectively). The three *Dunaliella* MLDP proteins are highly conserved in amino acid sequences with over 70% homology (but no homology in the nucleotide sequences).

A BLAST search in the National Center for Biological Information database of nonredundant proteins identified three orthologs: *Chlamydomonas reinhardtii* MLDP (accession number XP\_001697668), *Haematococcus pluviialis* HOGP (HQ213938) and *Volvox carteri* (XP\_002958653), all belonging to the Volvocales green algae lineage. A BLAST search in the National Center for Biological Information database of EST revealed lower level of homology to partial EST sequences of *Coccomyxa* sp. C-169 (GW222322), *Chlorella variabilis* (EFN52470), *Polytomella parva* (EC748417), *Prototheca wickerhamii* (EC182117) and *Micromonas pusilla* CCMP1545) XP\_003057303, also members of green algae lineage.

Multiple alignment of major oil globule proteins from *Dunaliella*, *C. reinhardtii* and *H. pluviialis* plus the putative *V. carteri* ortholog (Fig. 4), revealed that all proteins share a 21 amino acids conserved motif, which contains 4 prolines close to the C-terminal end (Fig. 4, highlighted). Surprisingly, these protein sequences show no homology to plant oleosins, to mammalian TAPs and not even to diatoms or to any other sequenced algae putative proteins, suggesting that MLDPs are unique to the green algal lineage.

A phylogenetic tree of MLDPs and putative orthologs was constructed by the neighbor-joining program in MEGA5 in order to identify their phylogenetic relationships (Fig. 5, Tamura et al. 2011). The analysis shows that *Dunaliella* MLDPs are most closely related to *H. pluviialis*, *C. reinhardtii* and *V. carteri*, belonging to the Volvocales, whereas *C. variabilis*, *Coccomyxa* sp., *P. wickerhamii* and *M. pusilla*, belonging to the Chlorellales, compose a different subgroup. These evolutionary relationships resembles the evolutionary pattern of green algae lineage without any exceptions (Handa et al. 2003; Nakada et al. 2008).

Kyte and Doolittle (1982) hydropathy plots and Grand average of hydropathy values (GRAVY) (Fig. 6I) revealed that even though the GRAVY vary significantly, from highly hydrophilic for *C. reinhardtii* (0.105), intermediate for *Dunaliella* (−0.016, −0.079 and −0.082 of *D. salina*, *D. bardawil* and *D. parva*, respectively) to hydrophobic for *H. pluviialis* (−0.157), all MLDPs share two conserved hydrophobic areas: One short region between amino acid residues 30 and 50, the second wide region approximately between amino acid residues 150 and 250. MLDPs differ in hydropathy profile from animal perilipin (Fig. 6If) and more so from plant oleosins, in lacking the central hydrophobic domain (Fig. 6Ig).

A secondary structure analysis (Guermeur et al. 1998) shows that all MLDPs are highly structured proteins, consisting mostly of  $\alpha$ -helices, and a short unstructured domain near the C-terminal end (Fig. 6II). This predicted structure of green algal MLDP greatly differs from plant oleosin, but resembles animal perilipin. It may be noted that the conserved 4-proline domain partly overlaps the unstructured loops domain.

#### Correlation between MLDP induction and TAG accumulation

To test if MLDP induction is correlated with TAG biosynthesis, we have followed the time course of MLDP mRNA and protein expression and of TAG accumulation during adaptation to N-deprivation. *D. salina* cells were grown either in complete or in N-deprived media for 14 days. Samples for RNA, protein extraction and oil accumulation were collected at the indicated times. Semi-quantitative PCR was performed to evaluate the expression levels of mRNA under N-deprivation (Fig. 7a). MLDP expression levels were compared with the expression levels of 18S control gene. The results revealed a biphasic increase in the amount of MLDP mRNA in N-deprived cells, one peaking at 24 h and a second increase after 7 days from the onset of nitrogen starvation. The first phase probably reflects the response to nitrogen deprivation and the second phase reflects entry to stationary phase, since it was correlated with complete growth arrest.

**Fig. 4** Multiple sequence alignment of *Dunaliella* MLDPs with other green algal orthologs. *D. salina*, *D. bardawil*, *D. parva*—this findings; other known MLDPs from *Chlamydomonas reinhardtii* (XP\_001697668), *Haematococcus pluvialis* (HQ213938) and *Volvox carteri* (XP\_002958653) genome. Identical residues are indicated by asterisks. Conserved areas are highlighted in gray. NCBI accession no. indicated in parentheses

C.reinhardtii	MAESA-----GKPLKHLEFVHTYAHKFASGAAYVEGG	32
D.bardawil	MAPKAVE-----KQQTP---SPGSQLRRLGWVRSVSTVASTAAPILGQ	40
D.parva	MAPASKTGPKGSTTPQAPTNTAGPQLRRLGFVRSYAGSAASLLAPILLT	50
D.salina	MAPKAVE-----KVVHP---PPGQLRRLAWVRSASSAAGLLAPVLGQ	40
H.pluvialis	MSE-----KQLKRLGFVHQGASAYSYTGTAEKL	29
V.carteri	MADD-----RKLKRLGFVDAYTHKLANGAAYVEGA	30
	*: *::* :*	
C.reinhardtii	YQKAKTYVPAVAQPYIAK-EETCLAYAAPLATKATDHAEKILRSTDAQLD	82
D.bardawil	VQHAGDLILE----RLGR-KEQLATYTAPLVLRAVDIGDAALNTLDQQVD	86
D.parva	VQSFQDRVLE----SVGT-KESLAAYTTPLEERTTDIGDLSLSTVDQQVD	95
D.salina	VQHVGDILE----RAGR-KEQLASYTTPLEKATDIDGDAALTSVDQQVD	85
H.pluvialis	YKTARSFAPTFVEPTLAQVEDRVVAITAPVVAQAQDLSEKALHIADDQVE	79
V.carteri	YKKVKPLVPQQVQPFLLAKVEDAVLAYTAPVVAKASDAQAEKFLRITDEQVD	80
	: . :: : ** : : * . : * * * :	
C.reinhardtii	ALYAASASWLSSS-----QKLADSNIAAFRGAADKYYDLVKSTA	121
D.bardawil	YVINTGSSAVGTAQQTIHDSANGVREIHSANLAFLNNAFQTYLTSLQQAT	136
D.parva	YMLNTGNSMVRTTSQTIVTDSVSGVRDIHNSNLSYLSNAFQTLTLLNLRQT	145
D.salina	YVISTGSAAVGTARQTI SDSANGVRDIHSANLAFLSNAFQTYLTSLQRT	135
H.pluvialis	CIVNTTDKAVADGKKGVIDCMNGVKEMHEKNMQTYIATSNRYFEYIKGMS	129
V.carteri	YLYVETAAYLTQT-----RKLTKSNIDTFRSAADKYYQMVKSTA	119
	: : : : * : : : : :	
C.reinhardtii	QHVTSKLPDLSVAKARELLSASLEQAKALADPDAAVAAALDAWTKFAAI	171
D.bardawil	DWAVENLNPVRASRAAWDWARATLARMQELLDPTLYNFLRERWAAFTSI	186
D.parva	DWAIENLNPVRIAHTGSDWAKATFVRAQELLDPTLYNFLQERWAAVSSI	195
D.salina	DWAVENLNPVRATRAAWDWARATLARMQELLDPTLNFNLRDRWAAFTSI	185
H.pluvialis	EWAKDKMNP I KGGQHALDTLNAAI AKAQEATDPDVAAKMALDANWSFASV	179
V.carteri	DYLASKLSYDISVQAARDFISKSVEKAKELSDPDAAVRIVYDSMQQFAAI	169
	: . :: : . : : : * : : : : :	
C.reinhardtii	PAAKVLVSAASPLTGKGVAAFTAHDLLVHVSALYRYGVSVGASTLWATS	221
D.bardawil	PVVRGVLDTVQPIITNAFWSIFYALHDFVVSGLYKFAVDSLSLSTWHWITD	236
D.parva	PVVKGMLDTAQPIITNASWSAFVGLHDFLVNSSLYKFSVDSGFSAWGWAKS	245
D.salina	PVVRGVLDTVQPIITNAFWNIIFYALHDFVVSWNLYKFAVDSLSLSTWHWITD	235
H.pluvialis	PVVAKVLETADPVTQTGLSSFYKLDHDLVSWPLYSKVSTGVSTLSWATT	229
V.carteri	PAAKTLEKTAPVTRKGFETFIAAHDALVSSLVYKRS-SLGATTLGMATT	218
	*. * * . * : * * * : * : * : * : : :	
C.reinhardtii	TPPYKLSAAYLYPLVQPVADPALDKVSKSTYVNAAIKYWAPAPV-----A	265
D.bardawil	SSPYKLGQYLYPIVQPVADPTLDKFAHSQVNSTLDYWKPN-----V	280
D.parva	TPPYKLGQYLYPIVQPVADPALHKVSSKVVNSVLDYWAPT PNAAAAAA	295
D.salina	SSPYKLGQYLYPIVQPVADPTLDKFTHSQVINSTLDYWKPN-----V	279
H.pluvialis	TMPYKLGQYMYPLVQPVADPALAKITNSKVINSTLSYWKPTA-----S	273
V.carteri	TPPYKLGQYLYPMVQSVADPALEKVAKSTYV NATLKYMAPV-----A	261
	: ****. * : * : * : * : * : * : * : * : * : * :	
C.reinhardtii	AA 267	
D.bardawil	VA 282	
D.parva	AS 297	
D.salina	VA 275	
H.pluvialis	AA 281	
V.carteri	AA 263	
	..	

To follow the protein level, anti-MLDP-specific polyclonal antibodies were generated in rabbits and utilized for western blot analysis. When tested with proteins of purified cytoplasmic globules, the anti-MLDP antibodies reacted specifically with a 30 kDa component (Fig. 7c). Pre-immune serum of the same rabbit did not give any reaction (data not shown). A time course of MLDP protein induction was conducted using total protein extracts from N-deprived cells

(Fig. 7b). As can be seen from the time course in 6b, MLDP protein level also increases in two phases, one starting at 24 h and decreasing after 72 h, and the second starting after 5.5 days. This kinetic response is correlated with the RNA expression, which also increases in two phases and drops in between after 96 h (Fig. 7a).

To monitor TAG accumulation, cells from control and from N-deprived cultures were stained with the fluorescent



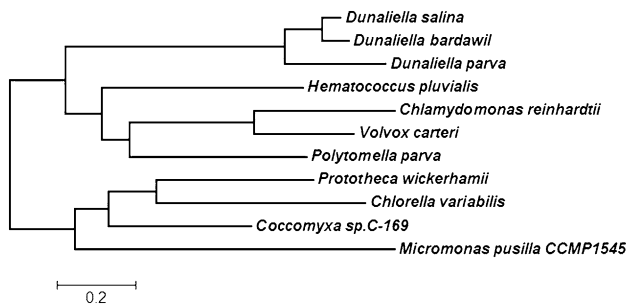


**Fig. 5** Phylogenetic tree of green algae MLDPs. The alignment was generated by the CLUSTAL W program and the phylogram was constructed by the neighbor-joining method using MEGA5 software (Tamura et al. 2011). MLDPs and orthologs (followed by NCBI accession numbers in parentheses): *Chlamydomonas reinhardtii* MLDP (XP\_001697668), *Hematococcus pluvialis* HOGP (HQ213938), *Volvox carteri* (XP\_002958653), *Coccomyxa* sp. C-169 EST (GW222322), *Chlorella variabilis* (EFN52470), *Polytomella parva* EST (EC748417), *Prototheca wickerhamii* (EC182117) and *Micromonas pusilla* CCMP1545 EST (XP\_003057303)

lipid indicator dye Nile red (NR) (Fig. 8a). The NR analysis indicated two kinetic phases in TAG accumulation in response to nitrogen deprivation, one peaking at 3 days and the second at 5.5 days. TLC analysis of lipid extracts revealed similar pattern (data not shown). This time course closely resembles the kinetics of MLDP protein accumulation (Fig. 7b). In contrast, control cells did not accumulate TAG. The cellular chlorophyll level in N-deprived cells dropped by about 50% already after 48 h, and further dropped after 7–8 days reflecting a large decrease in the level of the photosynthetic light harvesting and electron transport components (Fig. 8b). In contrast, the chlorophyll levels of control cells increased with time, probably reflecting shade adaptation resulting from increased cell density (Pick et al. 1987). These results are consistent with the results of confocal microscopy (Fig. 1).

#### MLDP expression depends on TAG biosynthesis

Because MLDP is a component of oil globules, it may be expected that inhibition of TAG biosynthesis might affect its induction. To check this possibility, we tested the effect of a TAG biosynthesis inhibitor on MLDP induction (Fig. 9). It has been previously reported that sethoxydim, an inhibitor of acetyl CoA carboxylase, inhibits TAG accumulation in *Dunaliella bardawil* (Rabbani et al. 1998). *D. salina* cells were grown in control medium or in N-deprived medium for 4 days. Sethoxydim was added at the onset of N-deprivation. Sethoxydim at 25–100  $\mu$ M did not significantly affect growth rates, but at 200  $\mu$ M inhibited growth by 30% (data not shown). As shown in Fig. 9, inhibition of TAG accumulation in *D. salina* by sethoxydim is

correlated with a parallel suppression of MLDP level, suggesting that MLDP biosynthesis is dependent on TAG accumulation.

#### Cellular localization of *D. salina* MLDP

Immunoelectron microscopy was utilized to identify the cellular localization of MLDP in algae grown under N-deprivation. Cells were fixed, cryosectioned, and immunolabeled first with anti-MLDP antibody followed by gold-conjugated goat anti-rabbit IgG. A comparison of control (Fig. 10a, b) with N-deprived cells (Fig. 10c, d) reveals a striking proliferation of starch granules in the latter, which occupy most of the chloroplast volume and replace the stacked thylakoid membranes. The N-deprived cells also contain cytoplasmic circular structures in the vicinity of the nucleus that we tentatively identified as lipid droplets (Glb). As shown in Fig. 10d and e, the gold immunolabel is concentrated at the periphery of these putative lipid droplets. No label could be observed in other cellular domains or in control cells, confirming that these structures are indeed lipid droplets.

#### Discussion

In this study, we describe the isolation and purification of cytoplasmic lipid droplets from the halotolerant alga *Dunaliella* and characterization of the major lipid droplet associated protein (MLDP) from three species of this alga. Although *Dunaliella* accumulates only moderate levels of TAG under N-deprivation in comparison to some green algae species, it is an ideal source for isolation of highly purified lipid droplets because it can be gently lysed by a mild osmotic shock which leaves the chloroplast intact, thus avoiding major contaminations of lipid droplets by pigments and hydrophobic proteins originating from the lysed chloroplast. Indeed, comparing the protein profile of purified globules from *D. salina* with those of *C. reinhardtii* (Moellering and Benning 2010), or with that from *H. pluvialis* (Peled et al. 2011) shows that both contain many additional proteins, most of which are probably contaminants from other cellular compartments. We have also added a novel control for identifying contaminating elements which are artificial lipid droplets prepared from synthetic triolein and trace phospholipids, which are added during cell lysis and supposedly adsorb released hydrophobic elements similar to natural lipid droplets. This is a valuable control in algae that require harsh treatments for cell lysis.

As mentioned above, *Dunaliella* contains also plastidic lipid droplets, which consist of  $\beta$ -carotene and TAG, which are present in small amounts in *D. salina* (Jiménez and Pick

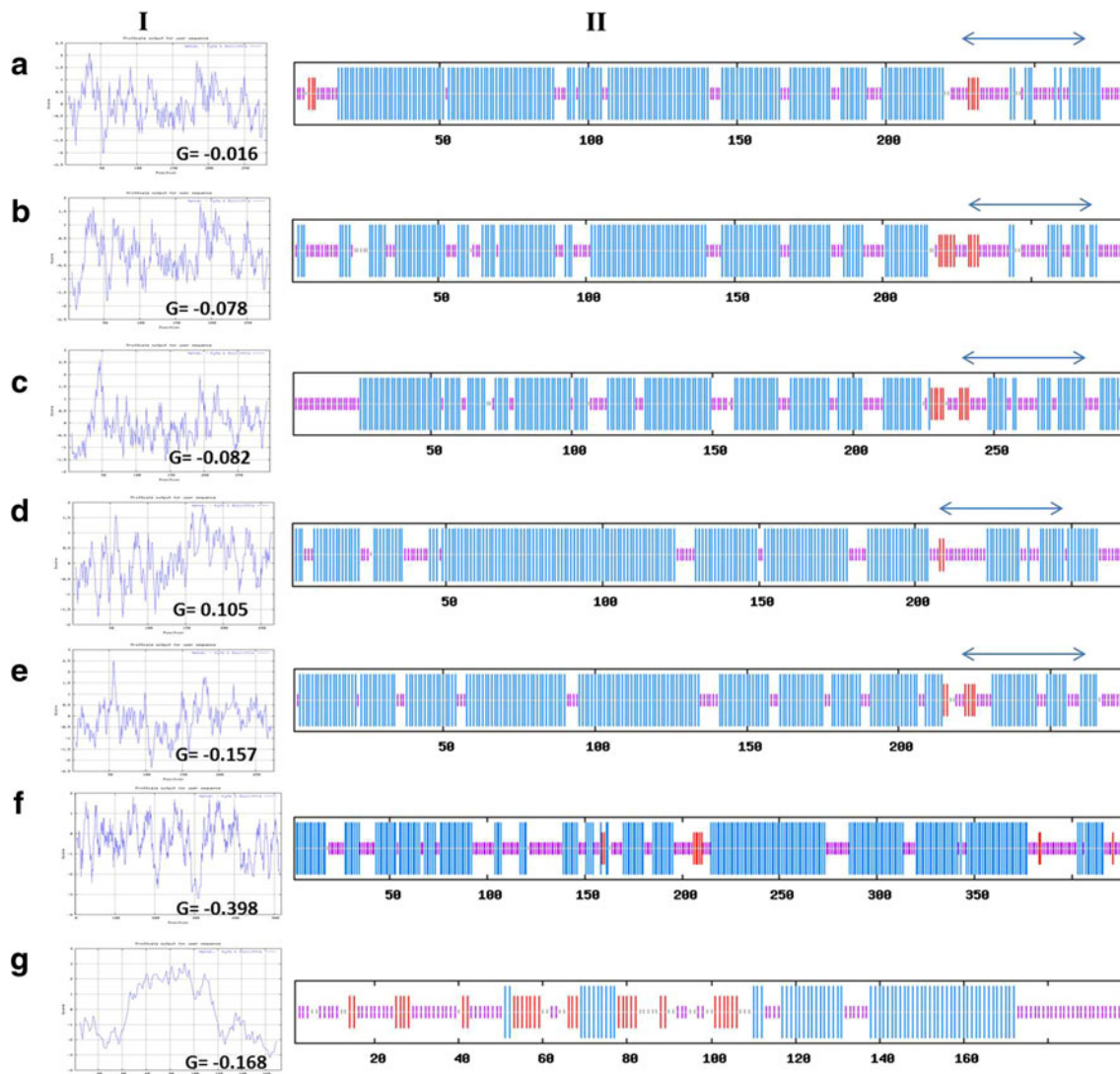


**Fig. 6** Hydropathy plot (*I*) and secondary structure prediction (*II*) of MLDP and other known lipid droplet-binding proteins. Secondary structure prediction was obtained by consensus secondary prediction program [http://npsa-pbil.ibcp.fr/cgi-bin/npsa\\_automat.pl?page=NPSA/npsa\\_server.html](http://npsa-pbil.ibcp.fr/cgi-bin/npsa_automat.pl?page=NPSA/npsa_server.html). Blue lines represent  $\alpha$ -helices, red lines represent extended strand, purple lines represent unstructured domains. **a** *D. salina* MLDP. **b** *D. bardawil* MLDP. **c** *D. parva* MLDP. **d** *Chlamydomonas*

*reinhardtii* MLDP (XP\_001697668). **e** *Haematococcus pluvialis* HOGP (HQ213938). **f** Mouse perilipin (NP\_783571). **g** *Arabidopsis thaliana* oleosin (NP\_194244.1). The NCBI accession numbers of each protein is indicated in parentheses. The *G* value in each graph is the GRAVY for each protein calculated using the GRAVY calculator program at <http://www.gravy-calculator.de>. The conserved 4-proline domain of MLDPs is marked with an arrow

1994), but are highly enriched in *D. bardawil* (Ben-Amotz et al. 1989). Differential isolation of cytoplasmic and plastidic lipid droplets may be achieved by sequential osmotic rupture of the plasma membrane followed by lysis of the chloroplast, as previously described (Jiménez and Pick 1994). Interestingly, the plastidic lipid droplets also contain a major lipid associated protein, of 38 kDa (Katz et al. 1995).

The fatty acid profile of lipid droplets from *D. salina* cells suggests that they differ from the rest of the cellular

fatty acids originating primarily from chloroplast membranes, as represented in control (DS + N) cells (Table 1). The fatty acid composition of N-deprived cells and more so of purified lipid droplets, shows a twofold increase in 16:0 and five- to eightfold increase, respectively, in 18:1 $\omega$ 9. The latter, which was also identified as a major constituent of lipid droplets in other green algae (Moellering and Benning 2010; Guarnieri et al. 2011; Peled et al. 2011), may be considered as a fatty acid marker for lipid droplets in green algae. These results indicate that the lipid droplets are

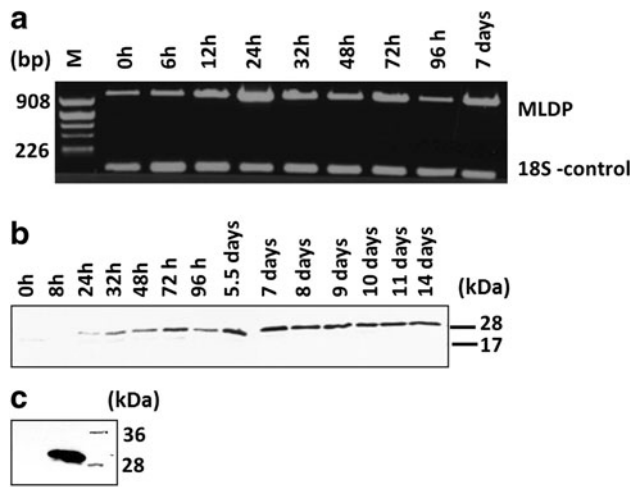


**Fig. 7** Expression of *D. salina* MLDP mRNA and protein. **a** mRNA expression. PCR was conducted on cDNA extracted from N-depleted cells at the indicated times, with MLDP complete gene-specific primers and 18S primers as control. *M* DNA marker. The results shown are representative of three experiments. **b** Protein expression. Western blot analysis of *D. salina* N-deficient cells during 14 days of culturing. Each lane contained proteins extracted from  $2 \times 10^6$  cells. Dilution of anti-MLDP antibody was 1:1,000. **c** Globule proteins. Western blot analysis on purified cytoplasmic globules with anti-MLDP antibodies (dilution 1:1,000). The results shown are representative of three experiments

composed of relatively saturated TAG (mainly 16:0 and 18:1 $\omega$ 9), which differ from the chloroplast galactolipids fatty acids, which are enriched in polyunsaturated fatty acids, mainly 16:4 $\omega$ 3 and 18:3 $\omega$ 3. The changes in fatty acid composition in N-depleted cells as compared to control cells, result both from the accumulation of saturated TAG in lipid droplets and from the massive degradation of the chloroplast membranes, reflected also by the decrease in cellular chlorophyll (Fig. 8b) (Kolber et al. 1988; Berges et al. 1996; Gaude et al. 2007). These results are consistent with previous reports in other unicellular alga that show that in most lipid-accumulating species, oil globules are characterized by a more saturated fatty acid composition in comparison to the polar lipid fatty acid composition (Guschina and Harwood 2006), although some microalgae are known to accumulate polyunsaturated FA (PUFA) in their TAG under stress conditions (Cohen et al. 2000; Harwood and Guschina 2009).

The deduced amino acid sequence of *D. salina* MLDP is about 70% identical to the *D. bardawil* and *D. parva* MLDPs. The three Dunaliella MLDPs together with the recently identifies MLDPs from *C. reinhardtii* (Moellering and Benning 2010), *H. pluvialis* (Peled et al. 2011) and green algal orthologs of *Volvox carteri* and *Polytomella parva* (partial sequence), all belonging to Volvocales order, seem to be part of a new gene family. There is no homology between Volvocales MLDPs neither with plant oleosins/

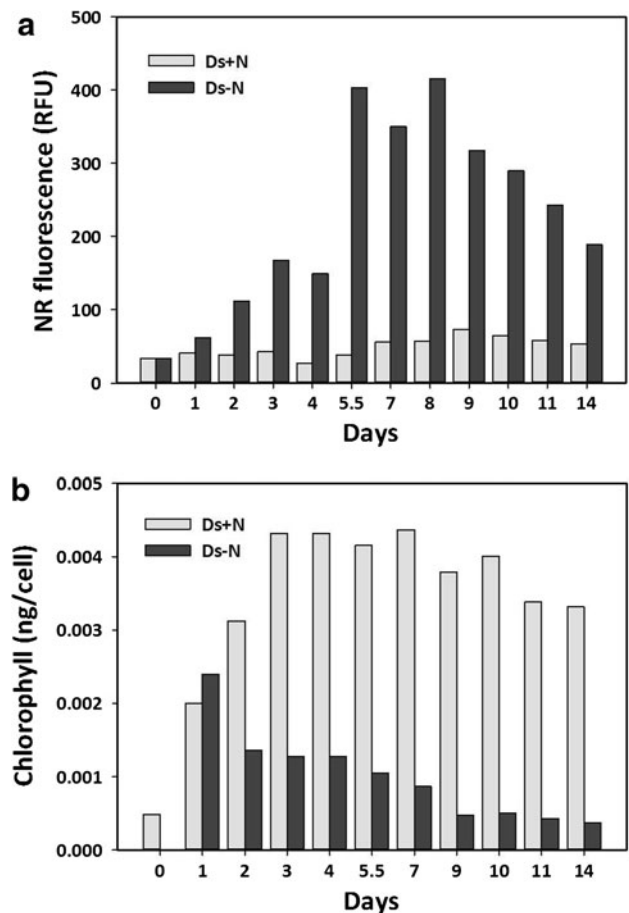


**Fig. 8** Quantification of *D. salina* TAG and chlorophyll. *D. salina* cells grown in complete (Ds + N) or in N-depleted (Ds – N) media for 14 days. **a** Quantification of TAG by NR fluorescence. **b** Quantification of chlorophyll levels in *D. salina* control and N-depleted cells. The results shown are representative of three experiments

caleosins, nor with animal perilipins, not in the primary structure and not in the hydropacy profile, suggesting that these families of proteins, which probably serve similar functions, evolved from different protein ancestors. Alignment of the MLDPs (Fig. 4) shows high sequence homology particularly in a highly conserved domain close to the C-terminal region that contains four conserved prolines (shaded).

A wider screen in NCBI database revealed additional orthologs with lower sequence homology to Volvocales MLDPs. They include *Coccomyxa* sp. C-169 (GW222 322), *Chlorella variabilis* (EFN52470), *Prototheca wickerhamii* (EC182117) and *Micromonas pusilla*, all belonging to the Chlorellales order. A phylogenetic tree of MLDPs proteins (Fig. 5) reveals that Volvocales MLDPs and putative Chlorellales MLDPs belong to different sub-families. The latter group did not share the 4-proline domain (data not shown).

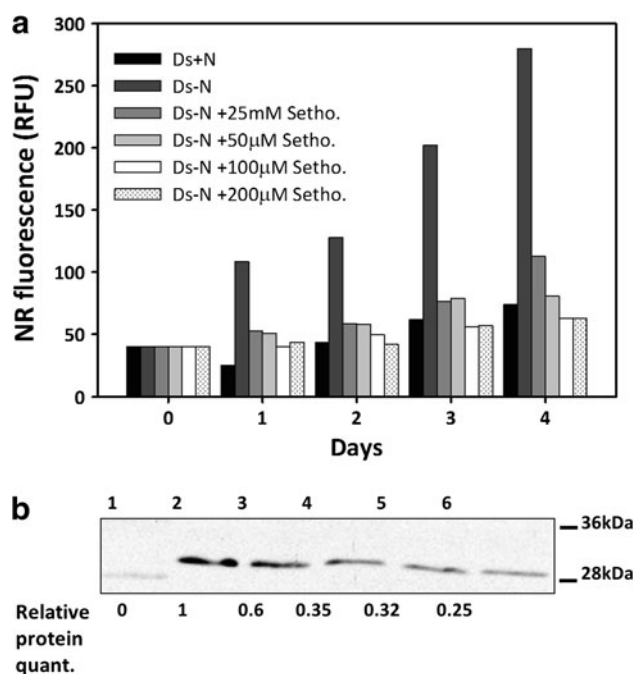


**Fig. 9** Effects of sethoxydim. The algae were cultured for 4 days in complete (Ds + N) or in N-deficient (Ds – N) media, with or without the indicated concentrations of sethoxydim. **a** TAG accumulation was quantified by NR fluorescence. **b** Western blot analysis of protein cell extracts with anti-MLDP antibody. Protein quantification values were calculated relative to Ds – N expression. 1 Ds + N, 2 Ds – N, 3 Ds – N + 25 1 M sethoxydim, 4 Ds – N + 50 1 M sethoxydim, 5 Ds – N + 100 1 M sethoxydim, 6 Ds – N + 200 1 M sethoxydim

The conserved 4-proline motif of Volvocales MLDPs was not found in any other known protein and it does not resemble the “proline knot”—the hallmark of plant oleosins and caleosins (Frandsen et al. 2001). An intriguing question for a protein that is associated with an oil body is, what are the domains that anchor the protein in the lipid. In plant oleosins/caleosins, the central large hydrophobic domain fulfills this role. In animal perilipins, three conserved slightly hydrophobic regions—H1, H2 and H3—were shown to be involved in targeting and anchoring the proteins to the lipid droplet (Garcia et al. 2003; Subramanian et al. 2004). Dunaliella and the homologs MLDPs are mostly mildly hydrophobic proteins and possess no gross hydrophobic domains. Using software for prediction of post-translational modifications revealed no putative conserved sites for palmitoylation, prenylation, myristoylation or GPI-anchor for the green algal MLDPs, ruling out the possibility of a post-translational lipid anchor. However, a close inspection of the hydropathy plots, discloses two conserved mildly hydrophobic domains that could serve a similar function to that of animal perilipins: a short domain (of 20–30 AA) between AA 30 and 70 and a longer domain (of

around 50 AA) between AA 150–230, which coincides with the unstructured domain (Fig. 6), and partly overlaps the conserved 4-proline motif. In future studies we plan to test if one of these domains and/or the 4-proline motif, contribute to the association of these proteins with lipid globules.

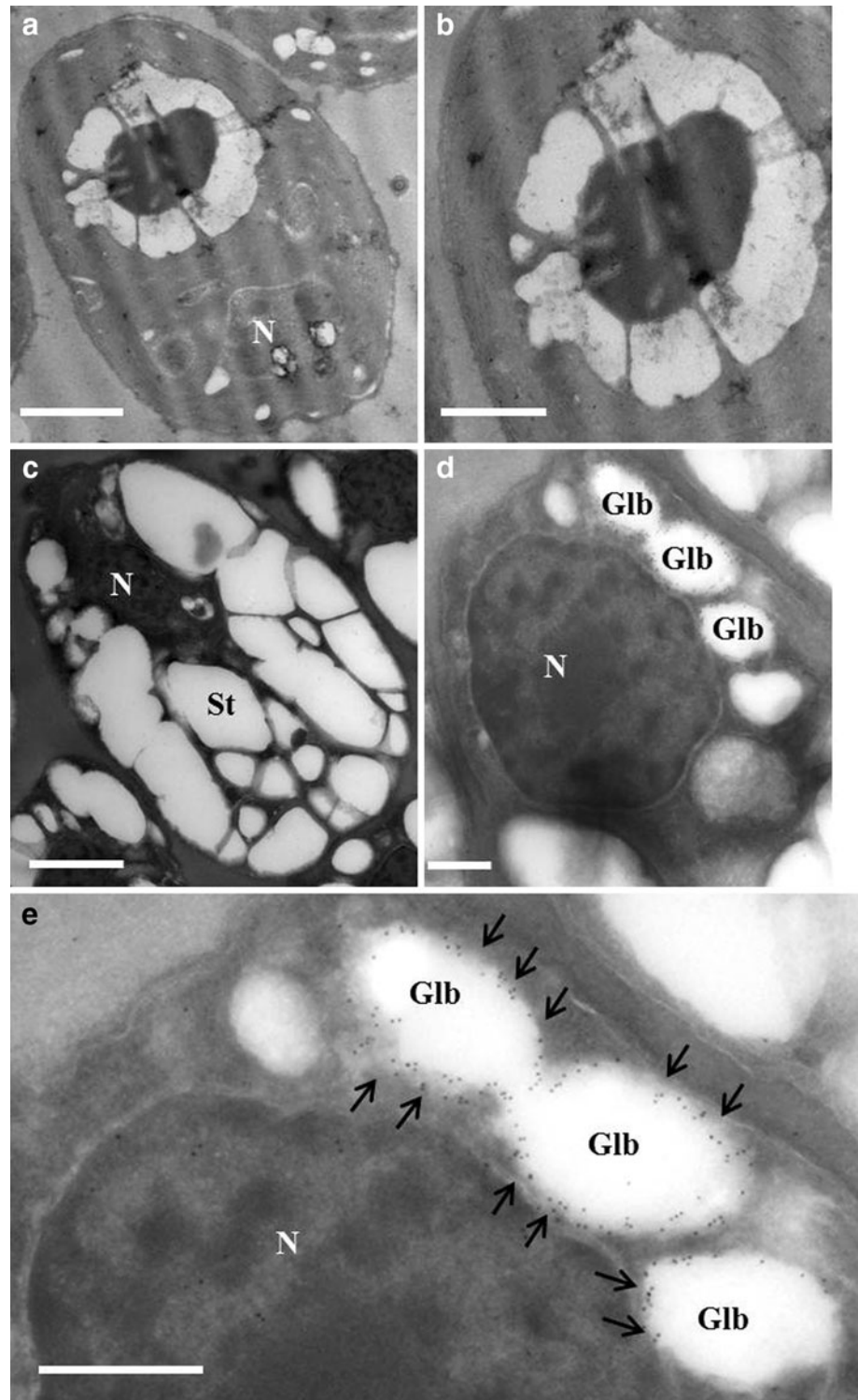
In mammalian perilipin, it has been shown that phosphorylation of several serine residues causes structural changes that initiate the lipolysis process of the droplet TAG through the interaction between perilipin to lipases (Ducharme and Bickel 2008). All MLDPs share three conserved Ser residues in their sequences that may function as potential phosphorylation site for controlling lipolysis in algal lipid droplets.

Evaluation of neutral lipid content in cells by NR fluorescence (Fig. 8a) revealed an eightfold increase in TAG levels in N-deprived cells compared to control cells. The biphasic induction of MLDP mRNA and protein (Fig. 7a, b), and the parallel accumulation of TAG (Fig. 8a), has not been previously observed in TAG accumulation in other algae and it clearly indicates two stages of stress. The first, 24–48 h from the onset of N-deprivation, probably results from growth retardation as the cells adapt to limiting nitrogen. This adaptation is associated also with a decrease in chlorophyll (Fig. 8b), in stacked membranes in the chloroplasts and in starch accumulation (Fig. 10) and in inhibition of protein synthesis (not shown). Cell division is retarded, but not stopped. The second stage (after 5–7 days) is correlated with complete growth arrest and probably reflects entry to the stationary phase. It is associated with a further two- to threefold increase in both MLDP protein and TAG level and a further decrease in chlorophyll.

The observation that MLDP biosynthesis is suppressed by inhibition of TAG accumulation suggests that TAG and MLDP biosynthesis are co-regulated which is not surprising in view of the fact that MLDP is an integral part of lipid droplets and since both are most probably synthesized in the endoplasmic reticulum. It is interesting to note that a similar co-regulation between biosynthesis of  $\beta$ -carotene and of TAG, which co-localize in plastidic lipid droplets in *D. bardawil*, was reported previously (Rabbani et al. 1998).

In this article, we introduced MLDP from three *Dunaliella* strains, presented the correlation between MLDP expression and oil accumulation in the N-deprived cells and localized MLDP to the lipid droplet periphery. This work strengthens the relation between oil accumulation and MLDP expression and indicated MLDP as a potential marker for identification of oil production. Nevertheless, further work should be done concerning the interaction between the protein and the globules, the structure of this protein family and their function in the cell.

**Fig. 10** Gold immunolabeling of *D. salina* MLDP by electron microscopy. The algae were grown for 3 days in complete or in N-deficient growth media. **a, b** Control cells. **c–e** N-deficient cells. *Glb* cytoplasmic globules, *St* starch, *N* nucleus. Arrows indicate MLDP. Bars 2  $\mu\text{m}$  (**a, c**), 1  $\mu\text{m}$  (**b**), 500 nm (**d, e**)



**Acknowledgments** We are grateful to the following scientists at The Weizmann Institute of Science: Mr. Vladimir Kiss from the Department of Biological Chemistry for his assistance in the Confocal Microscopy studies, Dr. Eyal Shimoni from the Department of Chemical Research Support for his help in the Electron Microscopy analyses and Dr. Miriam Eisenstein, also from the Department of Chemical Research Support, for her assistance and advice in the bioinformatic

analysis. We are also grateful to Dr. Inna Khozin-Goldberg and to Prof. Zvi Cohen from The Ben-Gurion University for the GC–MS fatty acid analysis. This work was supported by The Alternative Energy Research Initiative Fund at The Weizmann Institute, by the Minerva Center: Photosynthesis under stress in changing world and by The Charles and Louise Gartner fund (to UP).

## References

- Abd El-Baky HH, El Baz FK, El-Baroty GS (2004) Production of antioxidant by the green alga *Dunaliella salina*. *Int J Agric Biol* 6:49–57
- Altschul SF, Madden TL, Schaffer AA, Zhang J, Zhang Z, Miller W, Lipman DJ (1997) Gapped BLAST and PSI-BLAST: a new generation of protein database search programs. *Nucleic Acids Res* 25:3389–3402
- Avron A, Ben-Amotz A (1992) *Dunaliella*: physiology, biochemistry and biotechnology. CRC Press, Boca Raton
- Ben-Amotz A, Katz A, Avron M (1982) Accumulation of  $\beta$ -carotene in halotolerant algae: purification and characterization of  $\beta$ -carotene-rich globules from *Dunaliella bardawil*. *J Phycol* 18:529–537
- Ben-Amotz A, Shaish A, Avron M (1989) Mode of action of the massively accumulated beta-carotene of *Dunaliella bardawil* in protecting the alga against damage by excess irradiation. *Plant Physiol* 91:1040–1043
- Berges JA, Charlebois DO, Mauzerall DC, Falkowski PG (1996) Differential effects of nitrogen limitation on photosynthetic efficiency of photosystems I and II in microalgae. *Plant Physiol* 110:689–696
- Bickel PE, Tansey JT, Welte MA (2009) PAT proteins, an ancient family of lipid droplet proteins that regulate cellular lipid stores. *Biochim Biophys Acta* 1791:419–440
- Cohen Z, Khozin-Goldberg I, Adlerstein D, Bigogno C (2000) The role of triacylglycerol as a reservoir of polyunsaturated fatty acids for the rapid production of chloroplastic lipids in certain microalgae. *Biochem Soc Trans* 28:740–743
- Ducharme NA, Bickel PE (2008) Lipid droplets in lipogenesis and lipolysis. *Endocrinology* 149:942–949
- Frandsen GI, Mundy J, Tzen JT (2001) Oil bodies and their associated proteins, oleosin and caleosin. *Physiol Plant* 112:301–307
- Froissard M, D'Andrea S, Boulard C, Chardot T (2009) Heterologous expression of AtClol1, a plant oil body protein, induces lipid accumulation in yeast. *FEMS Yeast Res* 9:428–438
- Garcia A, Sekowski A, Subramanian V, Brasaemle DL (2003) The central domain is required to target and anchor perilipin A to lipid droplets. *J Biol Chem* 278:625–635
- Gaude N, Brehelin C, Tischendorf G, Kessler F, Dormann P (2007) Nitrogen deficiency in *Arabidopsis* affects galactolipid composition and gene expression and results in accumulation of fatty acid phytol esters. *Plant J* 49:729–739
- Goujon M, McWilliam H, Li W, Valentin F, Squizzato S, Paern J, Lopez R (2010) A new bioinformatics analysis tools framework at EMBL–EBI. *Nucleic Acids Res* 38:W695–W699
- Guarnieri MT, Nag A, Smolinski SL, Darzins A, Seibert M, Pienkos PT (2011) Examination of triacylglycerol biosynthetic pathways via de novo transcriptomic and proteomic analyses in an unsequenced microalga. *PLoS One* 6:e25851
- Guermeur Y, Paugam-Moisy H, Gallinari P (1998) Multivariate linear regression on classifier outputs: a capacity study. *Proceeding of ICANN'98*, pp 693–698
- Guo Y, Walther TC, Rao M, Stuurman N, Goshima G, Terayama K, Wong JS, Vale RD, Walter P, Farese RV (2008) Functional genomic screen reveals genes involved in lipid-droplet formation and utilization. *Nature* 453:657–661
- Guschina IA, Harwood JL (2006) Lipids and lipid metabolism in eukaryotic algae. *Prog Lipid Res* 45:160–186
- Handa S, Nakahara M, Tsubota H, Deguchi H, Nakano T (2003) A new aerial alga, *Stichococcus ampulliformis* sp. nov. (Trebouxiophyceae, Chlorophyta) from Japan. *Phycol Res* 51:203–210
- Harwood JL, Guschina IA (2009) The versatility of algae and their lipid metabolism. *Biochimie* 91:679–684
- Hsieh K, Huang A (2004) Endoplasmic reticulum, oleosins, and oils in seeds and tapetum cell. *Plant Physiol* 136:3427–3434
- Hu Q, Sommerfeld M, Jarvis E, Ghirardi M, Posewitz M, Seibert M, Darzins A (2008) Microalgal triacylglycerols as feedstocks for biofuel production: perspectives and advances. *Plant J* 54:621–639
- Huang AH (1992) Oil bodies and oleosins in seeds. *Annu Rev Plant Physiol Plant Mol Biol* 43:177–200
- Huang AH (1996) Oleosins and oil bodies in seeds and other organs. *Plant Physiol* 110:1055–1061
- Huesemann MH, Benemann JR (2009) Biofuels from microalgae: review of products, processes and potential, with special focus on *Dunaliella* sp. In: Ben-Amotz A, Polle JEW, Subba Rao DV (eds) *The alga Dunaliella: biodiversity, physiology, genomics, and biotechnology*. Science Publishers, Enfield, pp 445–474
- James GO, Hocart CH, Hillier W, Chen H, Kordbacheh F, Price GD, Djordjevic MA (2011) Fatty acid profiling of *Chlamydomonas reinhardtii* under nitrogen deprivation. *Bioresour Technol* 102:3343–3351
- Jiménez C, Pick U (1994) Differential stereoisomer compositions of  $\beta$ ,  $\beta$ -carotene in thylakoids and pigment globules in *Dunaliella*. *J Plant Physiol* 143:257–263
- Katz A, Jimenez C, Pick U (1995) Isolation and characterization of a protein associated with carotene globules in the alga *Dunaliella bardawil*. *Plant Physiol* 108:1657–1664
- Khozin-Goldberg I, Shrestha P, Cohen Z (2005) Mobilization of arachidonyl moieties from triacylglycerols into chloroplastic lipids following recovery from nitrogen starvation of the microalga *Parietochloris incisa*. *BBA* 1738:63–71
- Kolber Z, Zehr J, Falkowski P (1988) Effects of growth irradiance and nitrogen limitation on photosynthetic energy conversion in photosystem II. *Plant Physiol* 88:923–929
- Kyte J, Doolittle RF (1982) A simple method for displaying the hydrophobic character of a protein. *J Mol Biol* 157:105–132
- Moellering ER, Benning C (2010) RNA interference silencing of a major lipid droplet protein affects lipid droplet size in *Chlamydomonas reinhardtii*. *Eukaryot Cell* 9:97–106
- Murphy DJ (1993) Structure, function and biogenesis of storage lipid bodies and oleosins in plants. *Prog Lipid Res* 32:247–280
- Murphy DJ (2001) The biogenesis and functions of lipid bodies in animals, plants and microorganisms. *Prog Lipid Res* 40:325–438
- Nakada T, Misawa K, Nozaki H (2008) Molecular systematics of Volvocales (Chlorophyceae, Chlorophyta) based on exhaustive 18S rRNA phylogenetic analyses. *Mol Phylogenet Evol* 48:281–291
- Peled E, Leu S, Zarka A, Weiss M, Pick U, Khozin-Goldberg I, Boussiba S (2011) Isolation of a novel oil globule protein from the green alga *Haematococcus pluvialis* (Chlorophyceae). *Lipids* 46:851–861
- Pick U, Gounaris K, Barber J (1987) Dynamics of photosystem II and its light harvesting system in response to light changes in the halotolerant alga *Dunaliella salina*. 85:194–198
- Purkrtova Z, Jolivet P, Miquel M, Chardot T (2008) Structure and function of seed lipid-body-associated proteins. *C R Biol* 331:746–754
- Rabbani S, Beyer P, Lintig J, Huguency P, Kleinig H (1998) Induced beta-carotene synthesis driven by triacylglycerol deposition in the unicellular alga *Dunaliella bardawil*. *Plant Physiol* 116:1239–1248
- Rodolfi L, Chini Zittelli G, Bassi N, Padovani G, Biondi N, Bonini G, Tredici MR (2009) Microalgae for oil: strain selection, induction of lipid synthesis and outdoor mass cultivation in a low-cost photobioreactor. *Biotechnol Bioeng* 102:100–112
- Roessler PG (1990) Environmental control of glycerolipid metabolism in microalgae: commercial implications and future research directions. *J Phycol* 26:393–399

- Schenk P, Thomas-Hall S, Stephens E, Marx U, Mussgnug JH, Posten C, Kruse O, Hankamer B (2008) Second generation biofuels: high-efficiency microalgae for biodiesel production. *Bioenerg Res* 1:20–43
- Schmidt MA, Herman EM (2008) Suppression of soybean oleosin produces micro-oil bodies that aggregate into oil body/ER complexes. *Mol Plant* 1:910–924
- Shifrin NS, Chisholm SW (1981) Phytoplankton lipids: interspecific differences and effects of nitrate, silicate and light–dark cycles. *J Phycol* 17:374–384
- Siloto RM, Findlay K, Lopez-Villalobos A, Yeung EC, Nykiforuk CL, Moloney MM (2006) The accumulation of oleosins determines the size of seed oilbodies in *Arabidopsis*. *Plant Cell* 18:1961–1974
- Subramanian V, Garcia A, Sekowski A, Brasaemle DL (2004) Hydrophobic sequences target and anchor perilipin A to lipid droplets. *J Lipid Res* 45:1983–1991
- Tamura K, Peterson D, Peterson N, Stecher G, Nei M, Kumar S (2011) MEGA5: molecular evolutionary genetics analysis using maximum likelihood, evolutionary distance, and maximum parsimony methods. *Mol Biol Evol* 28:2731–2739
- Thompson GA Jr (1996) Lipids and membrane function in green algae. *Biochim Biophys Acta* 1302:17–45
- Tzen JT, Huang AH (1992) Surface structure and properties of plant seed oil bodies. *J Cell Biol* 117:327–335
- Zweytick D, Athenstaedt K, Daum G (2000) Intracellular lipid particles of eukaryotic cells. *Biochim Biophys Acta* 1469:101–120